A flexible multi-torus solar island concept

Trygve Kristiansen, Mari V. Sigstad, Jonathan Winsvold, Øyvind Rabliås and Odd M. Faltinsen
Department of Marine Technology, Norwegian University of Science and Technology (NTNU), Trondheim, Norway,
*trygve.kristiansen@ntnu.no

We propose a possible marine platform based on several concentric, flexible circular tori as support structure for floating solar islands (Figure 1). The tori are connected by pre-tensioned elastic bands. The structure will support a membrane deck that can carry light-weight cargo (such as solar panels) in waves. The main idea behind the concept is that it follows the waves to a large extent, thereby reducing need for airgap and offering a cost-efficient marine platform alternative. Several islands can be moored in framework type of mooring systems such as to cover large areas. Preliminary wave-tank experiments indicate that the concept is promising.

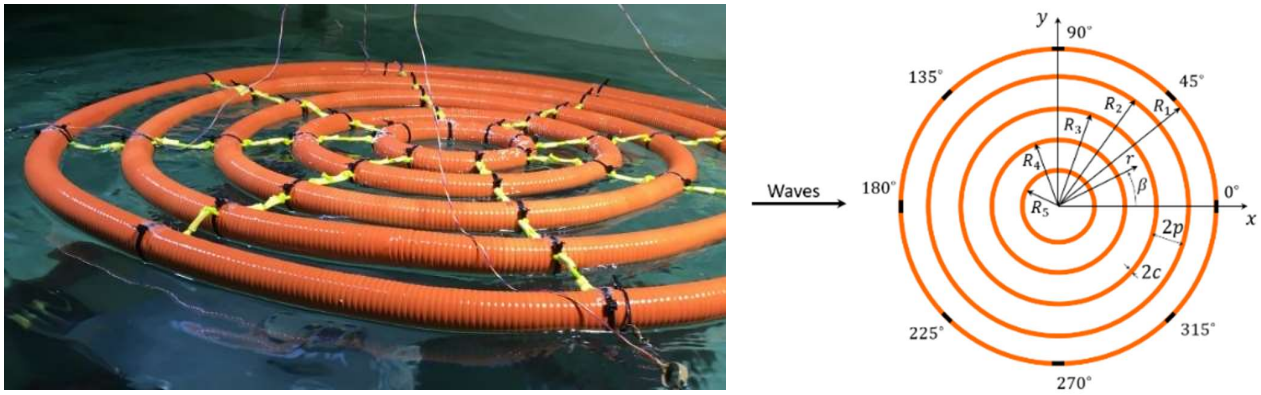

Figure 1. Multi-torus solar island model. Left: Preliminary experiments at NTNU 2018 and 2019. $2R_1 = 1\text{m}$. Cross-sectional diameter $2c = 0.032\text{m}$. Torus axis-to-axis distance $2p = 0.05\text{m}$. $EI = 0.847\text{Nm}^2$. *Right: Sketch with parameter explanations. The coordinate system is right-handed, such that the* $z-$*axis is positive upwards, and the origin is at the still water level. Waves travel along the positive* $x-$*axis.*

Although the structure follows vertically even quite steep regular waves very well, tests in irregular seas shows that over-topping occurs. Also, present results and published [1] shows that non-negligible super-harmonic accelerations occur. These may induce resonant flexible motions of the deck, for instance. This motivates development of a rational, combined hydrodynamic and structural model of the multi-torus system. The present text presents a step towards this.

Theory. The tori are coupled both structurally and hydrodynamically. We consider vertical motions only; heave, pitch, and flexible modes. The hydrodynamic interaction between the tori is investigated theoretically by means of extending the zero-frequency limit theory [2] to express the hydrodynamic interaction in terms of generalized cross-term added mass loads and generalized wave excitation loads. Vertical motion w_k are assumed small relative to R_k such that we can represent the vertical motion w_k of each torus $k = 1,..,K$ by a series of orthogonal modes,

$$w_k(\beta, t) = \sum_{n=0}^{\infty} a_{k,n}(t)\cos n\beta. \tag{1}$$

We model each torus by the modified Euler beam model [3],

$$m_k\frac{\partial^2 w_k}{\partial t^2} + EI_k\frac{\partial^4 w_k}{\partial s^4} + \frac{EI_k}{R_k^2}\frac{\partial^2 w_k}{\partial s^2} - \frac{\partial}{\partial s}\left(T_{ax,k}\frac{\partial w_k}{\partial s}\right) = f_k - 2\rho g c_k w_k. \tag{2}$$

Here $m_k = 0.5\rho\pi c_k^2$ is the structural mass per unit length of the torus, EI_k the bending stiffness, and f_k represent the external forces on torus k; wave excitation loads, added mass loads and point loads by elastic bands and moorings. $T_{ax,k}(s)$ is the axial tension in the torus, caused by mooring lines and connecting bands. The (hydrostatic) restoring load is given explicitly as $-2\rho g c_k w_k$. We assume that all tori have the same cross-sectional diameter c, mass per unit length m and bending stiffness EI in the following. By multiplying with $\cos m\beta$ and integration from 0 to 2π we decouple the modes,

$$m\ddot{a}_{k,n} - \sum_{j=1}^{K} a_{k,j,n}\ddot{a}_{j,n} + \frac{EI}{R_k^4}(n^4 - n^2)a_{k,n} + 2\rho g c\, a_{k,n} = f_{k,n}^{gen.}, \tag{3}$$

where $f_{k,n}^{gen}$ is the generalized load representing the wave loads and connecting bands. We have neglected the axial tension term to save space. In the following we assume steady-state solutions $b_{k,n} = \Re\left(a_{k,n}e^{-i\omega t}\right)$. The incident deep-water wave

velocity potential is given by $\phi_0(r,\beta,z,t) = \frac{g\zeta_a}{\omega} e^{kz}(\sum_{n=0}^{\infty} i^n \alpha_n J_n(kr)\cos n\beta) e^{-i\omega t}$, where $\alpha_0 = 2$ and $\alpha_{n\geq 1} = 1$. ζ_a is the incident wave amplitude, ω the wave frequency and J_n Bessel functions of the first kind and order n.

Radiation problem. We use the far-field solution by [2]. This is based on a slender-body approximation, justified by $c/R_k \ll 1$. Due to the zero-frequency limit approximation, the vertical motions of torus j are source-like, and the far-field flow is represented by a three-dimensional source distribution in the center-axis $z = 0, r = R_j$. The undisturbed pressure at torus k is then given by

$$\phi_j^F(R_k,\beta,0) = \frac{Q_{j,n}R_j}{4\pi}\int_0^{2\pi} \frac{\cos n\beta_0}{\left(R_k^2 + R_j^2 - 2R_kR_j\cos(\beta-\beta_0)\right)^{0.5}}\,\mathrm{d}\beta_0, \tag{4}$$

where the source strength amplitude $Q_{j,n} = 4c\dot{a}_{j,n}$ was found by an asymptotic expansion and matching between near- and far-field approximations. The flow induced by the vertical torus motion is source-like, so that the flow induced in the far-field is *horizontal* at $z = 0$. Due to the slenderness of the tori, torus k will experience a uniform (oscillating) current and behave as a horizontal dipole. We can therefore neglect the disturbances it causes and integrate the (undisturbed) pressure $p_j = -\rho\partial\varphi_j^F/\partial t$ multiplied with the modal shape $\cos n\beta$ of torus $k \neq j$ to obtain the (coupled added mass) load induced on it, and the added mass coefficients become

$$a_{k,j,n} = \frac{2}{\kappa_n\,\pi^2}\,\rho c^2 R_j \int_0^{2\pi}\int_0^{2\pi} \frac{\cos n\beta_0\cos n\beta}{\left(R_k^2 + R_j^2 - 2R_kR_j\cos(\beta-\beta_0)\right)^{0.5}}\,\mathrm{d}\beta_0\,\mathrm{d}\beta, \tag{5}$$

where $\kappa_0 = 1$ and $\kappa_{n\geq 1} = 2$. For $k = j$ we use the added mass as obtained by the single torus theory [2]. The integral is solved numerically. Note that orthogonality of modes implies *no hydrodynamic interaction between different modes*, i.e., motion in mode n of torus j will induce loads on torus k in mode n only. Therefore, the added mass coefficients are indexed by n only. This fact reduces the computational effort.

Diffraction problem. The diffraction force involves a (linear) boundary value problem with body velocity equal to minus the incident wave velocity, and there is therefore a hydrodynamic interaction load due to the other tori, similarly as for the radiation problem. The zero-frequency limit wave excitation loads is

$$f_{k,n}^{ex.gen} = \zeta_a \frac{1}{\alpha_n\pi}\left(2\rho g c\, J_n(kR_k) - \omega^2 \sum_{j=1}^{K} a_{k,j,n}\,\alpha_n\, J_n\big(kR_j\big)\right) i^{n+1} e^{-i\omega t}, \tag{6}$$

The connecting bands. We represent the point loads acting on torus k by a sum of Dirac delta functions $\sum_l P_{k,l}\delta(s_l)$, where $P_{k,l}$ is the point load and $s_l = R_k\beta_l$. It is important that the delta function has unit as the inverse of its argument, and that $\delta(s_l) = \delta(R_k\beta_l) = \delta(\beta_l)/R_k$. The point loads are modelled as the pre-tension $T_{p,l}$ multiplied by the local angle $\alpha_l = \left(w_k(\beta_l,t) - w_j(\beta_l,t)\right)/2(p-c)$,

$$P_{k,l} \simeq -T_p\,\frac{w_k(\beta_l,t) - w_j(\beta_l,t)}{2(p-c)},$$

assuming the bands stay pre-tensioned. Assuming Hooke's law, the vertical restoring loads due to elasticity of the bands will introduce loads proportional to α_l^3 only and are therefore negligible. Assuming steady-state solutions, we finally obtain the equations of motion for each torus k and for each mode n,

$$\left[-\omega^2\left(m + \sum_j a_{k,j,n}\right) + \frac{EI}{R_k^4}(n^4 - n^2) + 2\rho g c\right] b_{k,n} + \frac{T_p}{2(p-c)\pi R_k}\sum_n \frac{1}{\alpha_n}\left(b_{k,n} - b_{j,n}\right)\sum_l \cos n\beta_l \cos m\beta_l = f_{k,n}^{ex.gen.}. \tag{7}$$

All modes of all tori are coupled here. However, analyzing the sum over l, given the present arrangement of connecting bands, modes $n = 0, 1$ and 2 (heave, pitch and first flexible mode) are coupled with mode $n = 8, 7$ and 6 and some higher modes, respectively. Assuming motions of modes $n \geq 6$ are small, we can obtain separate systems of K equations for each of the modes heave and pitch, meaning coupled equations of motions for K tori, but without coupling with other modes.

Results. We first present results for the zero-frequency limit added mass. We use a case study that corresponds with the experiments indicated in Figure 1 which has $K = 5$ tori with torus radii $R_k = [25 - (k-1)5]$ m and cross-sectional radius $c = 0.8$ m. Added mass terms are presented as function of mode number n in Figure 2. The zero-frequency theory is in general in good agreement with the numerical simulations using a higher-order BEM version of WAMIT. The agreement is best for the off-diagonal terms. This show that the assumptions we made behind the zero-frequency limit is valid for this case. Also, the results illustrate that the hydrodynamic interaction is not negligible.

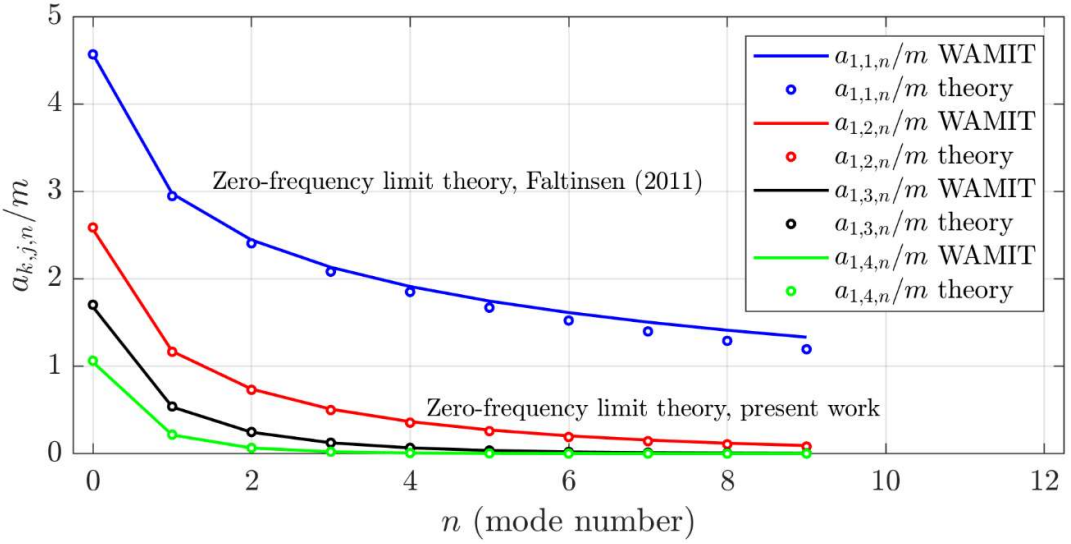

Figure 2. Zero-frequency limit non-dimensional added mass $a_{k,j,n}/m$ for the outer torus $k = 1$. The blue curve represents the diagonal added mass [2]. The red, black and green curves represent the cross-coupling added mass terms for the outer torus 1 due to forced motion of torus $j = 2, 3$ and 4, respectively.

However, the zero-frequency limit theory is not sufficient for analysis of the motions, except for large wavelength-to-torus diameter ratios, say $kR_1 < \sim 1.5$. Examples of normalized added mass, damping, wave excitation and motion RAOs for heave and the first flexible mode of the outer torus 1 are presented in Figure 3. Damping coefficients are not presented for clarity. There are similar strong frequency-dependency on added mass for the multi-torus as previously reported for single torus by [4] as one can expect, although shifted in frequency. It is intriguing that the lowest cancellation wave number in the RAOs (A) differ from that of the wave excitation forces. The reason is the hydrodynamic coupling between the tori.

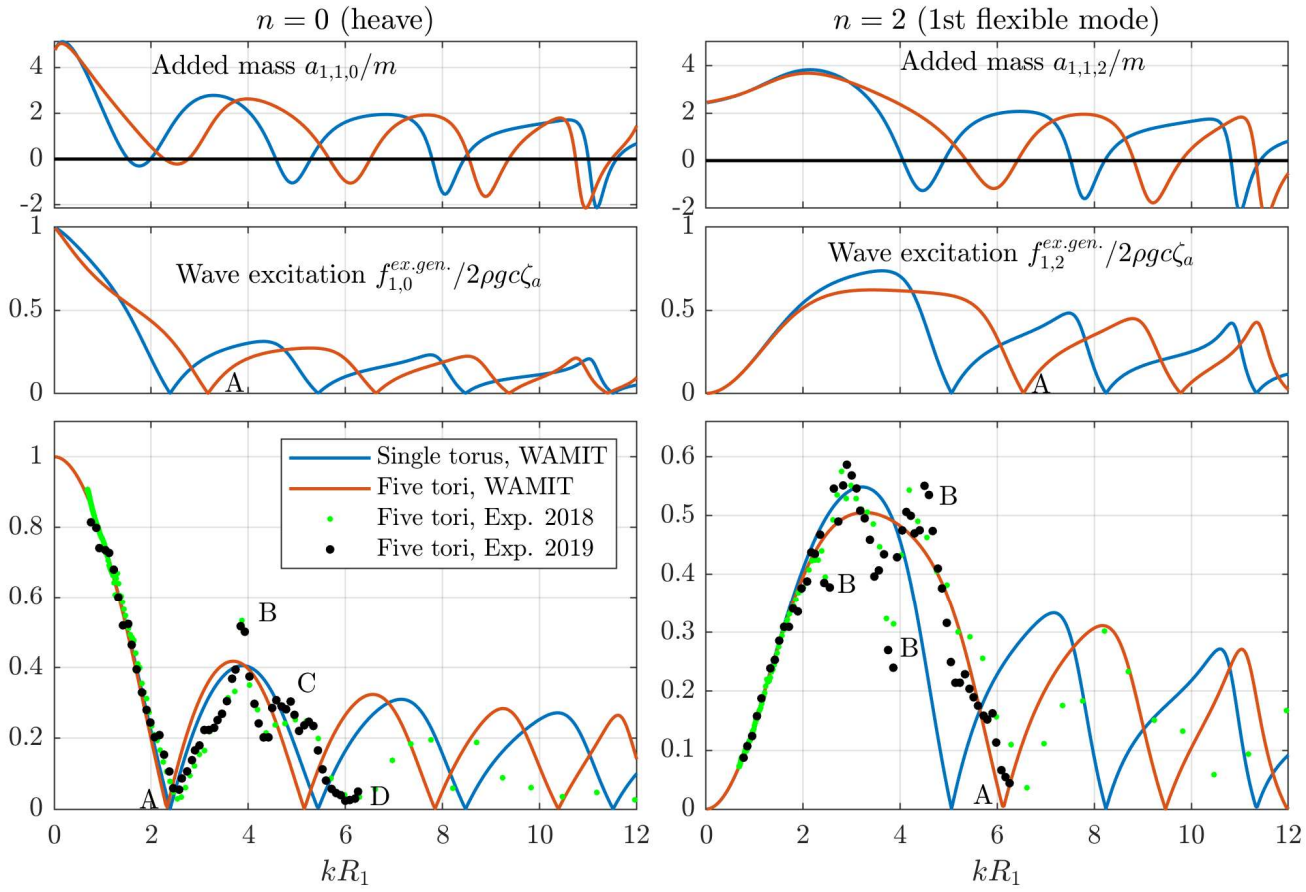

Figure 3. Non-dimensional added mass, wave excitation and motion RAOs as obtained by WAMIT for a single torus with the same properties as the outer torus 1, and outer torus 1 of the five-torus case.

In the experiments, the model diameter was $2R_1 = 1$ m and the tank width 2.5 m. Some of the irregularities of the experimental RAOs marked (B) are caused by tank wall reflections. This is demonstrated in Figure 4, where WAMIT simulations with tank walls are included. It is important to note that there *is* hydrodynamic coupling between modes in case of tank walls; all even modes $n = 0,2,4, \ldots$ are coupled due to symmetry around the yz −plane, and all odd modes $n = 1,3,5, \ldots$ are coupled due to anti-symmetry around the same plane. This means all odd or even modes must be considered simultaneously.

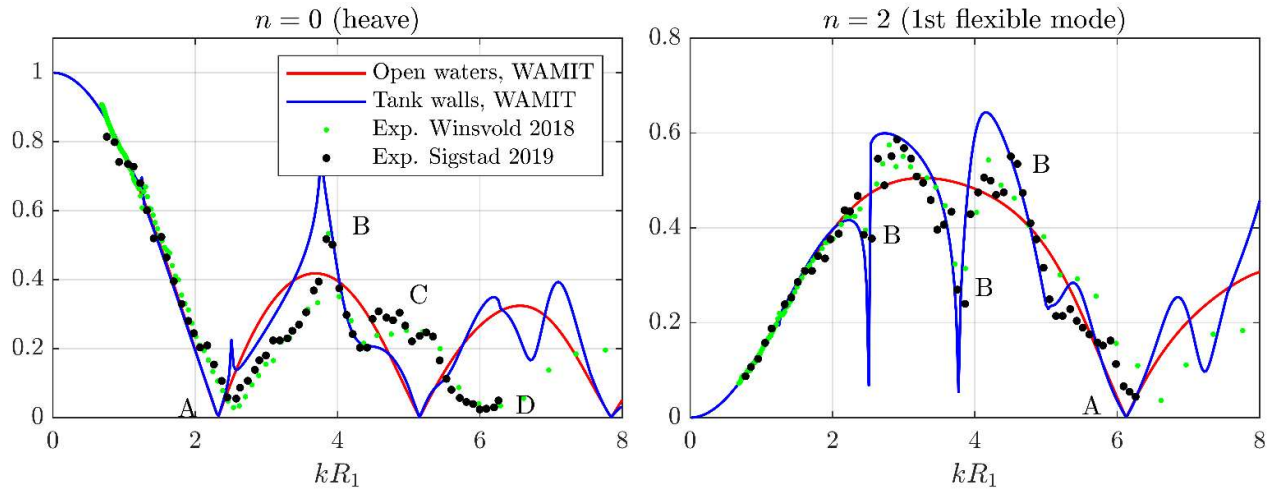

Figure 4. Motion RAOs in heave and the first flexible mode of the outer torus. Simulations with and without tank walls.

The hump marked by (C) and shift indicated by (D) are not explained by tank wall effects. The connecting bands represent one candidate. The heave RAO of torus 1 as predicted by (7) with $T_p = 1$N model scale (scale 1:50) is presented in Figure 5. The bands cause a clear shift. However, the shift is not as large as in the experiments, and a larger pre-tension is not thought realistic. Further, it does not predict the shift at (E). For pitch and the first flexible mode (not shown), the effect of the connecting bands is very small.

Another candidate to the discrepancies (C, D) is coupling effects with horizontal modes. There is a non-negligible hydrodynamic coupling between surge and pitch for $kR_1 > \sim 3$, despite the low draft. A flexible radial motion that is proportional to $\cos n\beta$ will cause a pressure field proportional to this mode shape (in open waters). This will cause a hydrodynamic load on the vertical mode $\cos n\beta$. We have not yet investigated this but will attempt so by including also horizontal flexible modes in WAMIT in further work.

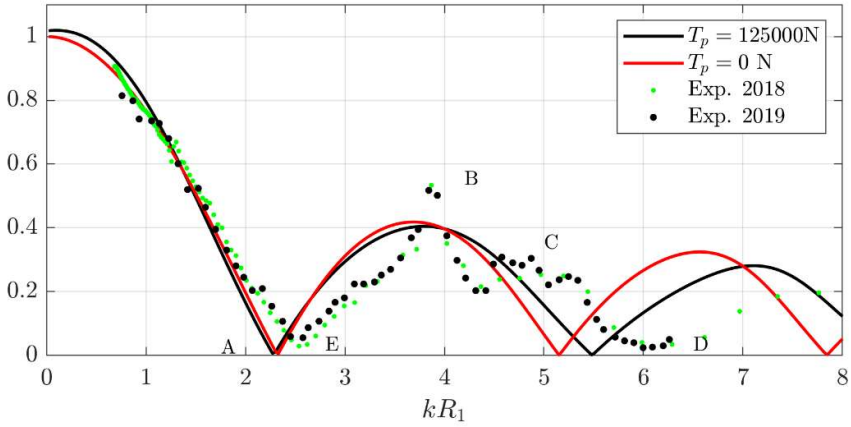

Figure 5. Heave RAO of outer torus 1, with and without connecting bands as in Eqn. (7).

The axial term in (2) will cause so-called Hoop stresses which contribute dynamically. One can account for these in a rational manner as in [2]. This must also be investigated as a possible cause. Waves of wave steepness $H/\lambda = 1/30$ and $1/60$ were tested to investigate the effect of wave nonlinearity, but the RAOs are very similar. The wave steepness plays a role in over-topping, which is mainly a consequence of the nonlinearity of the incident wave and nonlinear wave diffraction and radiation by the tori. We emphasize that tank wall effects are of importance and must be accounted for.

[1] Peng Li, O. M. Faltinsen and M. Greco. *Wave-Induced Accelerations of a Fish-Farm Elastic Floater: Experimental and Numerical Studies*. J. Offshore Mech. Arctic Engng. 140, 1 (2017)

[2] O. M. Faltinsen. Hydrodynamic aspects of a floating fish farm with circular collar. 26th IWWWFB, Athens (2011)

[3] T. Kristiansen and O. M. Faltinsen. *Experimental and numerical study of an aquaculture net cage with floater in waves and current.* J. Fluids Struct. 54 (2015)

[4] Peng Li. A theoretical and experimental study of wave-induced hydroelastic response of a circular floating collar. PhD thesis NTNU (2016)